Transient Buffering Effects of Parks Accessibility Against Movement Control Policies on Child Weight Status: A Quasi-Experimental Analysis in Singapore

Lucas Shen[1,*]; Ka Kei Sum[1,2]; Michelle Z.L. Kee[1]; Mya Thway Tint[1,3]; Evelyn C. Law[1,3,4]; Fabian Yap[5]; Yung Seng Lee[4]; Yap-Seng Chong[1,6,7]; Keith M. Godfrey[8]; Jonathan Y. Huang[5,9,*]

Affiliations: [1] Institute for Human Development and Potential, Agency for Science, Technology and Research, Singapore; [2] Population Health Sciences, Bristol Medical School, University of Bristol, United Kingdom; [3] Human Potential Translational Research Programme, Yong Loo Lin School of Medicine, National University of Singapore, Singapore; [4] Department of Paediatrics, Yong Loo Lin School of Medicine, National University of Singapore, Singapore; [5] Duke–NUS Medical School, National University of Singapore, Singapore; [6] Yong Loo Lin School of Medicine, National University of Singapore, Singapore; [7] Department of Obstetrics and Gynaecology, National University Health System, Singapore; [8] MRC Lifecourse Epidemiology Centre and NIHR Southampton Biomedical Research Centre, University of Southampton and University Hospital Southampton NHS Foundation Trust, United Kingdom; [9] Thompson School of Social Work and Public Health, University of Hawai'i at Mānoa, Honolulu, United States

Correspondence*: Lucas Shen; Jonathan Y. Huang, Email(s): lucas_shen@a-star.edu.sg; jon.huang@hawaii.edu.

Funding/Support: The GUSTO study is supported by the National Research Foundation (NRF) under the Open Fund–Large Collaborative Grant (OF-LCG; MOH-000504) administered by the Singapore Ministry of Health's National Medical Research Council (NMRC) and the Agency for Science, Technology and Research (A*STAR). In RIE2025, the study is supported by funding from the NRF's Human Health and Potential (HHP) Domain, under the Human Potential Programme. KMG is supported by the UK Medical Research Council (MC_UU_12011/4) and the National Institute for Health and Care Research (NIHR Senior Investigator (NF-SI-0515-10042) and NIHR Southampton Biomedical Research Centre (NIHR203319)). For the purpose of Open Access, the author has applied a Creative Commons Attribution (CC BY) licence to any Author Accepted Manuscript version arising from this submission.

Ethics: Ethical approval for the GUSTO cohort (0–9 years) was granted by the Domain Specific Review Board (DSRB) [D/2009/00021] and the Centralised Institutional Review Board (CIRB) [2018/2767/D]. Ethical approval for the GUSTO follow-up (10 years onwards) was provided by the CIRB and DSRB [2019/2655/E]. Informed parental consent was obtained for all participants.

Conflict of Interest: The authors declare no competing interests.

Data & Code Availability: All code for analyses will be made publicly available. Requests for access to GUSTO data can be submitted to the GUSTO Data Access Committee and will be reviewed in accordance with institutional and ethical guidelines.

Abbreviations: BMI, body mass index; GUSTO, Growing Up in Singapore Towards healthy Outcomes; COVID-19, coronavirus disease 2019; SD, standard deviation; CI, confidence interval; WHO, World Health Organization

Keywords: Child adiposity; Park accessiblity; Built environment; Outdoor play; Difference-in-differences, Natural experiment; GIS

Date: January 6, 2026

Word count (main text): 1515 (via auto `texcount`)

Abstract word count: 166 (via auto `texcount`)

Abstract

Background

Evidence linking neighborhood environments to health is typically observational. We use quasi-experimental variation from COVID-19 to estimate whether hyperlocal park access buffered children against obesogenic effects.

Methods

Longitudinal adiposity outcomes are from the Growing Up in Singapore Towards healthy Outcomes cohort (n = 964, ages 9–10 in 2020, 9,984 child-year observations, 2010–2024), including BMI, weight, zBMI, skinfolds, and fat mass, with height as placebo. Park access measures parks reachable within 10 minutes using travel time and annual land inventory. We estimate an event-study difference-in-differences model with child and neighborhood-year fixed effects.

Results

In 2020, children with high park access experienced a relative decline in BMI (-0.37 kg/m^2, 95% CI: $[-0.672, -0.071]$). Differences attenuated to zero by 2023 (0.02 kg/m^2, 95% CI: $[-0.570, 0.613]$). We find no pre-trends. Patterns mirrored across adiposity measures, but not height. High access associated with lower probability of outdoor play cessation (-12.7 percentage points, 95% CI: $[-24.2, -1.3]$).

Discussion

Higher park access muted obesogenic effects of movement restrictions during COVID-19, with evidence supporting preserved outdoor play as a behavioral mechanism.

1 Background

Neighborhood environments, particularly access to parks, may play a crucial role in promoting healthy child development, including obesity prevention.[1–9] However, such effects are challenging to identify due to confounding structural and individual-level forces that drive residential location.[3,5,8,10,11] Moreover, contextual and age-specific factors that influence how children engage with the built environment suggest that acute policy changes can have widely varying effects.[8,11,12]

In previous work, we found that a large proportion of Singaporean children stopped outdoor play following COVID-19 lockdowns and had correspondingly higher adiposity one year later.[12] However, it was not clear whether such trends would persist,[12,13] nor what built environment features might protect children against these effects. For children living in residential areas with a good number of parks reachable within a short journey, opportunities for outdoor and physical play may remain available.[1,3,8,9,12]

This study builds on recent evidence of pandemic-related outdoor play[12] and increased parks use.[9] We use COVID-19-related movement restrictions as a natural experiment to investigate a policy-relevant question: Does park accessibility around the time of an acute policy shock that disincentivized outdoor play buffer school-aged children against any potentially lasting adverse effects on adiposity? To investigate this, we combine novel, constructed spatio-temporal data on park accessibility with longitudinal repeated measures of adiposity and longitudinal residential histories spanning up to four years post-lockdown.

2 Methods

2.1 Cohort and Anthropometric Measures

We leverage 12,829 standardized anthropometric measures across 15 years (2010–2024) for 1,176 children from the Growing Up in Singapore Towards health Outcomes (GUSTO) study,[14] a geographically-representative mother-offspring cohort (Appendix A).[15] Anthropometric outcomes include BMI (kg/m^2), weight (kg), and height (cm), measured by clinically-trained study

staff. We also report zBMI measures, as well as skinfold thickness and fat mass for a smaller subset (Appendix F). Since 2024 observations are sparse and occur early in the year, we bin them with 2023 in the event study.[16]

2.2 Park Access

We measure residential park access for each child by linking residential histories, an annual inventory of areas zoned as parks, and commute times based on a grid of 0.1 km^2 hexagons (Appendix A). Commute times were computed using routing engines based on pedestrian networks and public transport schedules.[17] We exclude serial movers (who relocated twice or more),[10] resulting in a final sample of 964 children and 9,984 child-year observations. Annual residence is assigned based on the closest record before birthdays. Park access was dichotomized as above (high access) or below (low access) the mean number of parks reachable within a 10-minute walk or public transit ride from home postcode.

2.3 Difference-in-Differences Design

The quantity of interest is the difference between the two groups (high versus low park access) after the onset of COVID-19 (vertical gap in Figure A2). We formally estimate these group differences using dynamic difference-in-differences (DiD),[18] adjusting for time-invariant child factors, developmental age-specific trends, and neighborhood-year effects under the assumption that trends across neighborhoods would otherwise be similar except for any differential effects of the lockdown.[10,19,20] Differences between groups are relative to the difference in 2019 as the baseline year.[16,18,19] We clustered the standard errors by child to account for within-individual correlation across time for asymptotically valid inference.[19,21–23] Importantly, DiD does not require an absence of selection bias, only that it be time-invariant.[16,19] Instead, a key assumption is that, absent COVID-19, both groups' outcomes would have followed the same trajectory (Appendix B).[16,18,19]

2.4 Sensitivity Analyses

To test the DiD assumption, we verify that pre-COVID differences are null in all pre-COVID years across all outcomes.[16,18,19] We analyze weight, zBMI, skinfold measures, and fat mass to evaluate consistency across anthropometric outcomes (Appendix F). We analyze height as a negative control outcome, since it should not respond to short-run shocks. Any differences here would suggest residual confounding. Additionally, we consider a (wide) two-period DiD estimator,[18] using the closest measurements before and after the first lockdown (Appendix E).

2.5 Outdoor Play

To evaluate a potential behavioral mechanism,[1,3,12] we link to a contemporaneous COVID-19 survey on outdoor play that elicited reports of outdoor play,[12] yielding $n = 310$ linked children (Appendix G). We measure whether there was any outdoor play before and during the pandemic, and whether there was a complete cessation of outdoor play (from any play to none) during this period. As a placebo, we test pre-COVID differences in outdoor play. Differences would imply selection on pre-existing outcomes, while nulls would support the interpretation that parks helped preserve spaces for child outdoor play.

3 Results

In March 2020, GUSTO child ages ranged from 8.8 to 10.3 years (mean 9.5, SD 0.36; Figure A3). Among children with high park access (n = 237) in 2020, the mean (SD) number of parks within a 10-minute journey was 6.5 (SD 4.5), and the mean BMI was 18.5 (SD 4.1). For those with low park access (n = 388), the corresponding values were 0.7 (SD 0.8) parks and a BMI of 18.8 (SD 4.2).

In 2020, there was a relative BMI decline for those with high park access ($\hat{\gamma}_{2020} = -0.372$ kg/m^2, 95% CI: $[-0.672, -0.071]$; Figure 2a; Table D1). However, this difference between groups attenuated toward the 2019 baseline by 2021 ($\hat{\gamma}_{2021} = -0.197$ kg/m^2, 95% CI: $[-0.597, 0.203]$), with similarly small, statistically indistinguishable-from-zero estimates in 2022–2023 ($\hat{\gamma}_{2022} = 0.133$ kg/m^2, 95% CI: $[-0.388, 0.654]$; $\hat{\gamma}_{2023} = 0.022$ kg/m^2, 95% CI:

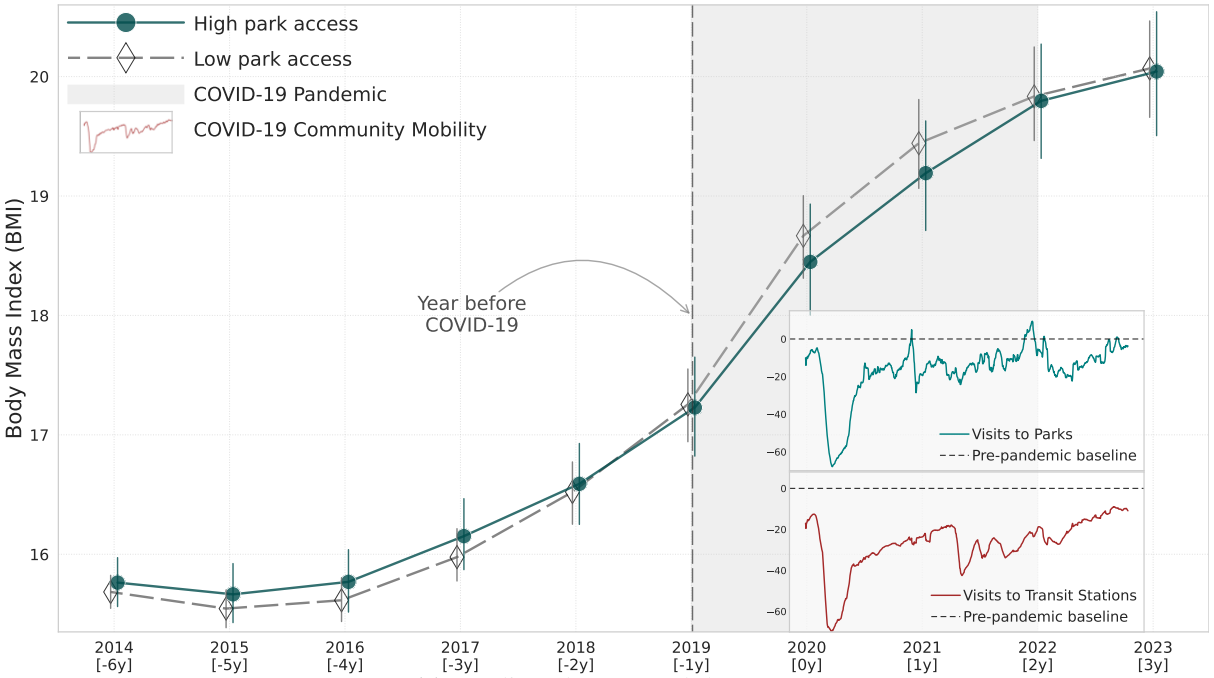

(a) Unadjusted BMI trends by group

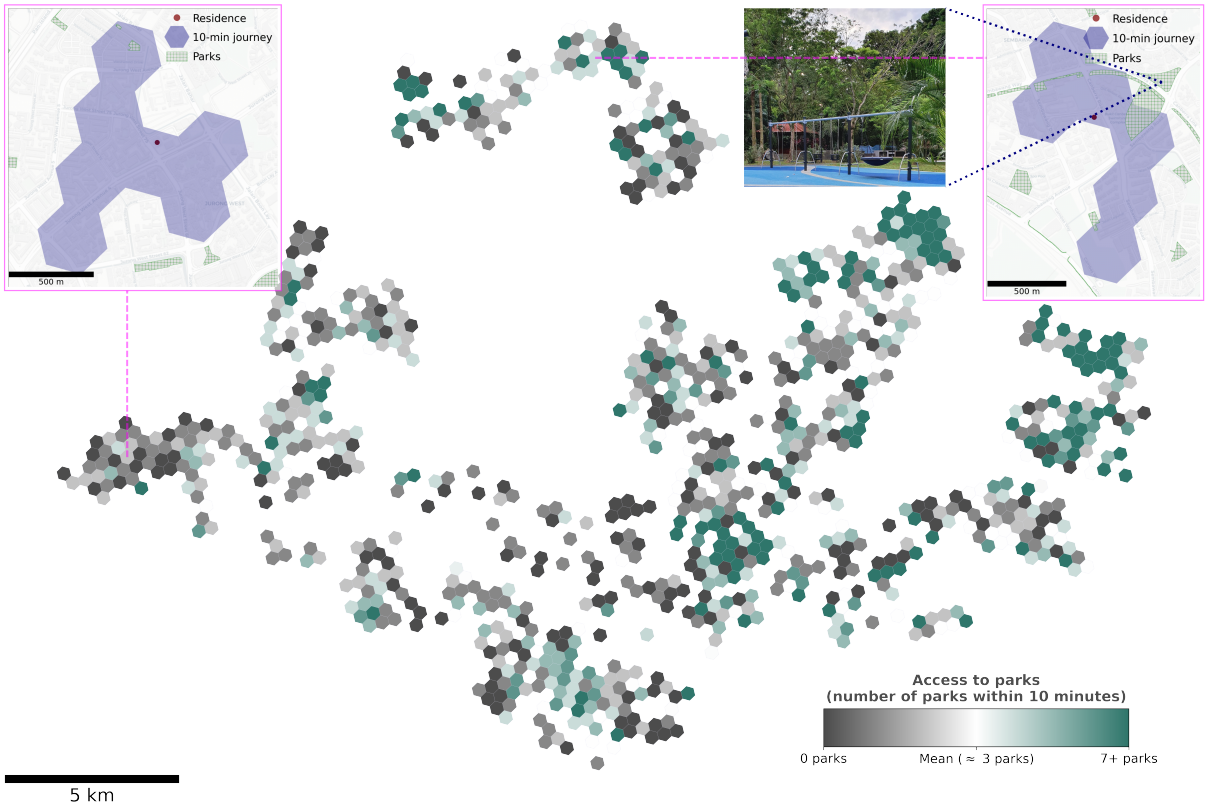

(b) Distribution of residential park access

Figure 1|BMI trends and spatial access to parks by group.
(a) Average unadjusted yearly BMI for children with high park access versus low park access. Vertical lines are 95% bootstrapped confidence intervals. Insets show COVID-19 Community Mobility trends from Google[24] (Appendix A) for visits to parks (top) and transit stations (bottom), aligned to the same time axis. The gray area bookends 2020–2021, when movement restrictions were in place. Brackets indicate years relative to the start of COVID-19 in 2020.
(b) Spatial distribution of park access across the study area, measured as the number of parks within a 10-minute walk. Insets illustrate low-access (left) and high-access (right) examples at higher resolution.

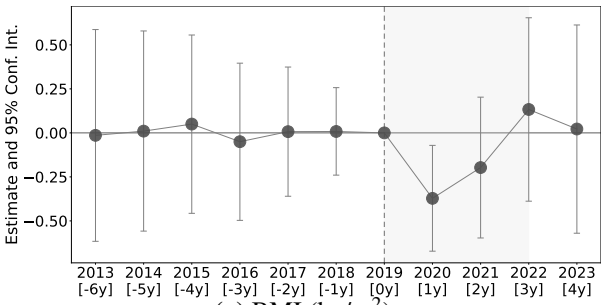

(a) BMI (kg/m^2)

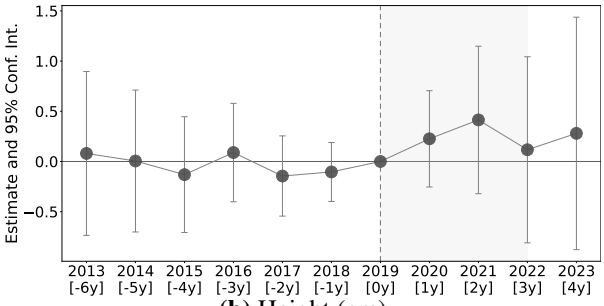

(b) Height (cm)

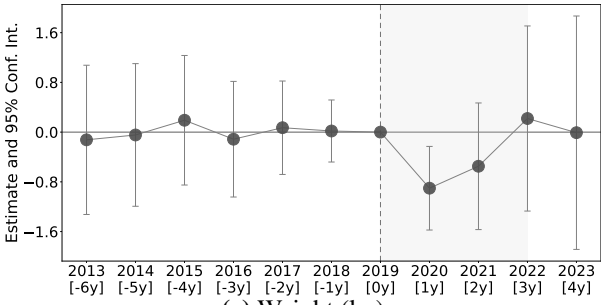

(c) Weight (kg)

Year	n	Age (SD)		BMI (SD)		Height (SD)		Weight (SD)	
2010	728	0.3	(0.3)	15.3	(2.4)	58.8	(8.4)	5.6	(2.2)
2011	885	1.1	(0.4)	16.5	(1.5)	75.2	(6.7)	9.4	(1.8)
2012	836	1.9	(0.4)	16.3	(1.5)	84.6	(4.7)	11.7	(1.7)
2013	803	2.8	(0.5)	15.9	(1.7)	93.0	(5.5)	13.8	(2.4)
2014	788	3.9	(0.6)	15.7	(2.0)	101.3	(5.8)	16.3	(3.1)
2015	769	5.0	(0.4)	15.6	(2.2)	108.9	(5.4)	18.7	(3.8)
2016	752	6.0	(0.4)	15.7	(2.5)	115.1	(5.5)	21.0	(4.6)
2017	730	7.0	(0.3)	16.1	(2.9)	121.1	(5.7)	23.9	(5.7)
2018	690	7.9	(0.5)	16.6	(3.3)	126.6	(6.5)	27.0	(7.2)
2019	666	8.9	(0.5)	17.3	(3.7)	132.4	(6.7)	30.8	(8.7)
2020	625	10.1	(0.4)	18.7	(4.2)	140.1	(7.4)	37.1	(10.6)
2021	608	11.1	(0.4)	19.5	(4.4)	146.5	(7.5)	42.2	(11.8)
2022	554	12.0	(0.5)	19.9	(4.4)	152.8	(8.0)	46.8	(12.6)
2023	483	12.8	(0.3)	20.0	(4.3)	157.8	(7.9)	50.2	(12.9)
2024	117	13.2	(0.2)	20.1	(4.0)	158.4	(7.5)	50.5	(11.8)

(d) Summary of data by year

Figure 2|Estimates of the dynamic difference-in-differences. Each point is the estimate ($\hat{\beta}_p$ and $\hat{\gamma}_q$) of the difference in the outcome between the children with high park access versus low park access relative to the difference in 2019 as the baseline year (the year before COVID-19), from estimating:

$$y_{it} = \alpha_i + \tau_t + \sum_{p=2010}^{2018} \beta_p \left(D_i \cdot \mathbb{1}\{t = p\}\right) + \sum_{q=2020}^{2023} \gamma_q \left(D_i \cdot \mathbb{1}\{t = q\}\right) + f(\text{Age}_{it}) + \eta_{s(i),t} + \varepsilon_{it}, \tag{1}$$

where i indexes children and $t \in \{2010, \ldots, 2023\}$ indexes calendar years (2024 binned into 2023), adjusting for time-invariant child effects (α), year trends (τ), a quadratic in age, and neighborhood-by-year effects ($\eta_{s(i),t}$). Capped vertical bars are 95% confidence intervals constructed from standard errors clustered by child. The COVID period is shaded in gray. Brackets indicate the year(s) relative to the start of COVID-19 in 2020. Tables D1 to D3 tabulate all estimates. The table reports summary statistics by year; means are reported with standard deviations (SD) in parentheses.

$[-0.570, 0.613]$).

Importantly, we find no pre-trends (Figures 2a to 2c). Pre-2020 coefficients were statistically zero across outcomes, indicating comparable pre-period trajectories with no underlying differences in outcome trends. For instance, the 2018 BMI difference was 0.008 kg/m^2 (95% CI: $[-0.240, 0.257]$; Figure 2a; Table D1), with prior-year estimates likewise indistinguishable from zero. We therefore interpret post-2020 estimates as reflecting the effects of higher park access.

The patterns in BMI are mirrored in weight (2020: −0.902 kg, 95% CI: $[-1.575, -0.230]$; 2021: −0.549 kg, 95% CI: $[-1.568, 0.469]$; 2022: 0.219 kg, 95% CI: $[-1.270, 1.708]$; Figure 2c) and zBMI (2020: −0.141, 95% CI: $[-0.259, -0.023]$; 2021: −0.113, 95% CI: $[-0.260, 0.034]$; 2022: 0.008, 95% CI: $[-0.172, 0.188]$; Appendix F), but not in height (2020: 0.226 cm, 95% CI: $[-0.254, 0.705]$; 2021: 0.414 cm, 95% CI: $[-0.321, 1.148]$; 2022: 0.117

cm, 95% CI: $[-0.810, 1.043]$; Figure 2b). Patterns were also similar with skinfold thickness and fat mass for a subset where the measures are available (Appendix F). We observe similar patterns with other land use as exposures (e.g., mixed residential/commercial zones, civic & community), but pre-COVID differences and trends violate DiD identifying assumptions, so we treat these as exploratory (Appendix H).

Results were similar using the two-period DiD estimator (Appendix E), where we find a relative decline in BMI (-0.224 kg/m^2, 95% CI: $[-0.469, 0.021]$), weight (-0.583 kg, 95% CI: $[-1.170, 0.007]$), zBMI (-0.082, 95% CI: $[-0.178, 0.015]$), but not height (0.14 cm, 95% CI: $[-0.25, 0.53]$) as a placebo outcome.

Finally, we examined changes in outdoor play (n = 310, Appendix G). 88% reported some outdoor play before COVID-19, but this fell to 57% during the pandemic. High park access was associated with a higher probability of outdoor play during the lockdowns (10.1 percentage points, 95% CI: $[-0.9, 21.0]$). Again, there are no pre-COVID differences in outdoor play between groups as placebo (-5.2 percentage points, 95% CI: $[-13.3, 2.9]$). Moreover, children with high park access had a lower probability of ceasing outdoor play (-12.7 percentage points, 95% CI: $[-24.2, -1.3]$).

4 Discussion

In our previous study, elimination of outdoor play time was associated with greater-than-average weight gain 1 year post COVID-19 lockdowns.[12] Here, we extend this finding, showing that park access around the time of the lockdowns reduced the risk of eliminating outdoor play as a behavioral mechanism[1,12] and that there was a commensurately lower (or less gain in) adiposity 1 year onward across various measures. Height as a placebo showed no differential changes, and pre-COVID differences were null across all outcomes, supporting the interpretation that high park access had anti-obesogenic effects.

However, such effects were short-lived, with the differences being largest during the first year (when movement constraints were most severe)[25–27] and attenuating thereafter. A behavioral model reconciles these patterns, grounding the natural experiment in a theory where

amenity usage depends on weighing health benefits against travel costs (Appendix C). COVID-19 effectively constrains usage to hyperlocal amenities by imposing additional costs of travel (e.g., infection risk, curtailed movement). Since these disincentives resolve with the loosening of control measures by 2022,[25,27] so too may any benefits. Alternatively, behavioral patterns established during lockdowns may be more persistent than any temporal changes brought about by the immediate built environment.

One limitation of this study is the lack of ground-truthing of actual park usage, so the findings should be interpreted as intent-to-treat. We also do not observe park quality. Moreover, we did not consider other moderating individual and family-level factors that facilitate usage. Future studies should examine ground-truth park use (e.g., sensors, GPS/diaries) and environmental exposures as multi-faceted, with potentially interacting effects. Nonetheless, intent-to-treat estimates align with planning levers, where cities can expand nearby amenities but not enforce usage.

The global prevalence of weight gain rose sharply during the 2020 pandemic.[12,13,28–33] We find benefits of park access on muting the obesogenic effects of unexpected shocks to movement and structured activities.[9] Supporting evidence suggests that nearby parks preserve spaces that facilitate outdoor play among early adolescents. As the first of its kind, our natural experimental evidence provides a narrowly-focused but potentially realistic estimate of one of the effects of built environments on child adiposity and is potentially useful for identifying which neighborhoods may be more resilient and to what extent, at least temporarily. It may also be relevant for families where accessing city-wide amenities is routinely constrained.

References

1 Floyd MF, Bocarro JN, Smith WR, Baran PK, Moore RC, Cosco NG, et al. Park-Based Physical Activity Among Children and Adolescents. American Journal of Preventive Medicine. 2011;41(3):258-65. Available from: https://www.sciencedirect.com/science/article/pii/S0749379711003278.

2 Wolch J, Jerrett M, Reynolds K, McConnell R, Chang R, Dahmann N, et al. Childhood obesity and proximity to urban parks and recreational resources: A longitudinal cohort study. Health & Place. 2011;17(1):207-14. Health Geographies of Voluntarism. Available from: https://www.sciencedirect.com/science/article/pii/S1353829210001528.

3 Nordbø ECA, Raanaas RK, Nordh H, Aamodt G. Neighborhood green spaces, facilities and population density as predictors of activity participation among 8-year-olds: a cross-sectional GIS study based

on the Norwegian mother and child cohort study. BMC Public Health. 2019 October;19(1):1426. Available from: https://doi.org/10.1186/s12889-019-7795-9.

4 Jia P, Cao X, Yang H, Dai S, He P, Huang G, et al. Green space access in the neighbourhood and childhood obesity. Obesity Reviews. 2021;22(S1):e13100. E13100 OBR-06-20-4551. Available from: https://onlinelibrary.wiley.com/doi/abs/10.1111/obr.13100.

5 Daniels K, Lê-Scherban F, Auchincloss AH, Moore K, Melly S, Razzaghi H, et al. Longitudinal associations of neighborhood environment features with pediatric body mass index. Health & Place. 2021;71:102656. Available from: https://www.sciencedirect.com/science/article/pii/S1353829221001520.

6 Jiang Q, Carlson JA, Kaczynski AT, Shook RP, Besenyi GM, Steel C, et al. Neighborhood park access and park characteristics are associated with weight status in youth. Health & Place. 2023;83:103116. Available from: https://www.sciencedirect.com/science/article/pii/S1353829223001533.

7 Daniels KM, Schinasi LH, Auchincloss AH, Forrest CB, Diez Roux AV. The built and social neighborhood environment and child obesity: A systematic review of longitudinal studies. Preventive Medicine. 2021;153:106790. Available from: https://www.sciencedirect.com/science/article/pii/S0091743521003595.

8 Ludwig J, Sanbonmatsu L, Gennetian L, Adam E, Duncan GJ, Katz LF, et al. Neighborhoods, Obesity, and Diabetes — A Randomized Social Experiment. New England Journal of Medicine. 2011;365(16):1509-19. Available from: https://www.nejm.org/doi/full/10.1056/NEJMsa1103216.

9 Geng DC, Innes JL, Wang G. Survive, revive, and thrive: The impact of COVID-19 on global park visitation. Science of The Total Environment. 2024;946:174077. Available from: https://www.sciencedirect.com/science/article/pii/S0048969724042256.

10 Finkelstein A, Gentzkow M, Williams H. Sources of geographic variation in health care: Evidence from patient migration. Q J Econ. 2016 Nov;131(4):1681-726. Available from: https://doi.org/10.1093/qje/qjw023.

11 Chetty R, Hendren N, Katz LF. The Effects of Exposure to Better Neighborhoods on Children: New Evidence from the Moving to Opportunity Experiment. American Economic Review. 2016 April;106(4):855–902. Available from: https://doi.org/10.1257/aer.20150572.

12 Sum KK, Cai S, Law E, Cheon B, Tan G, Loo E, et al. COVID-19–Related Life Experiences, Outdoor Play, and Long-term Adiposity Changes Among Preschool- and School-Aged Children in Singapore 1 Year After Lockdown. JAMA Pediatrics. 2022 03;176(3):280-9. Available from: https://doi.org/10.1001/jamapediatrics.2021.5585.

13 Ochoa-Moreno I, Taheem R, Woods-Townsend K, Chase D, Godfrey KM, Modi N, et al. Projected health and economic effects of the increase in childhood obesity during the COVID-19 pandemic in England: The potential cost of inaction. PLOS ONE. 2024 01;19(1):1-19. Available from: https://doi.org/10.1371/journal.pone.0296013.

14 Soh SE, Tint MT, Gluckman PD, Godfrey KM, Rifkin-Graboi A, Chan YH, et al. Cohort profile: Growing Up in Singapore Towards healthy Outcomes (GUSTO) birth cohort study. Int J Epidemiol. 2014 Oct;43(5):1401-9. Available from: http://dx.doi.org/10.1093/ije/dyt125.

15 Shen L, Raj S, Oulhote Y, Valvi D, Ng S, Lo SL, et al. Residential proximity to transport facilities as urban determinants of individual-level per- and poly-fluoroalkyl substance (PFAS) exposures: Analysis of two longitudinal cohorts in Singapore. Environmental Health. 2026. Accepted.

16 Freyaldenhoven S, Hansen C, Pérez JP, Shapiro JM. Visualization, Identification, and Estimation in the Panel Event-Study Design [Working Paper]; 2021. Available from: https://www.nber.org/papers/w29170.

17 HERE Technologies. HERE Routing API Documentation;. https://www.here.com/docs/category/routing.

18 Wang G, Hamad R, White JS. Advances in Difference-in-differences Methods for Policy Evaluation Research. Epidemiology. 2024;35(5). Available from: https://journals.lww.com/epidem/fulltext/2024/09000/advances_in_difference_in_differences_methods_for.6.aspx.

19 Roth J, Sant'Anna PHC, Bilinski A, Poe J. What's trending in difference-in-differences? A synthesis of the recent econometrics literature. Journal of Econometrics. 2023;235(2):2218-44. Available from: https://www.sciencedirect.com/science/article/pii/S0304407623001318.

20 Wang G, Hamad R, White JS. Advances in Difference-in-differences Methods for Policy Evaluation Research. Epidemiology. 2024;35(5). Available from: https://journals.lww.com/epidem/fulltext/2024/09000/advances_in_difference_in_differences_methods_for.6.aspx.

21 Wooldridge JM. Two-Way Fixed Effects, the Two-Way Mundlak Regression, and Difference-in-Differences Estimators; 2021. Preprint, August 16, 2021. Available from: https://www.researchgate.net/publication/353938385.

22 Goin DE, Riddell CA. Comparing Two-way Fixed Effects and New Estimators for Difference-in-Differences: A Simulation Study and Empirical Example. Epidemiology. 2023;34(4):535-43. Available from: https://journals.lww.com/epidem/fulltext/2023/07000/comparing_two_way_fixed_effects_and_new.11.aspx.

23 Rambachan A, Roth J. A More Credible Approach to Parallel Trends. The Review of Economic Studies. 2023 02;90(5):2555-91. Available from: https://doi.org/10.1093/restud/rdad018.

24 Google LLC. COVID-19 Community Mobility Reports; 2020. Available from: https://www.google.com/covid19/mobility/.

25 Ritchie H. Google Mobility Trends: How has the pandemic changed the movement of people around the world?; 2020. Https://ourworldindata.org/covid-mobility-trends. Available from: https://ourworldindata.org/covid-mobility-trends.

26 Cucinotta D, Vanelli M. WHO Declares COVID-19 a Pandemic. Acta Biomedica. 2020 March 19;91(1):157-60. Available from: https://doi.org/10.23750/abm.v91i1.9397.

27 Burki T. WHO ends the COVID-19 public health emergency. The Lancet Respiratory Medicine. 2023 Jul;11(7):588. Available from: https://doi.org/10.1016/S2213-2600(23)00217-5.

28 Gao L, Peng W, Xue H, Wu Y, Zhou H, Jia P, et al. Spatial–temporal trends in global childhood overweight and obesity from 1975 to 2030: a weight mean center and projection analysis of 191 countries. Globalization and Health. 2023 August 4;19(1):53. Available from: https://doi.org/10.1186/s12992-023-00954-5.

29 World Obesity Federation. Prevalence of Obesity;. Available from: https://www.worldobesity.org/about/about-obesity/prevalence-of-obesity.

30 Jenssen BP, Kelly MK, Powell M, Bouchelle Z, Mayne SL, Fiks AG. COVID-19 and Changes in Child Obesity. Pediatrics;147(5):e2021050123. Available from: https://doi.org/10.1542/peds.2021-050123.

31 Patterson RR, Sornalingam S, Cooper M. Consequences of COVID-19 on the Childhood Obesity Epidemic. BMJ;373(n953):n953. Available from: https://doi.org/10.1136/bmj.n953.

32 Rundle AG, Park Y, Herbstman JB, Kinsey EW, Wang YC. COVID-19-Related School Closings and Risk of Weight Gain Among Children. Obesity (Silver Spring);28(6):1008-9. Available from: https://doi.org/10.1002/oby.22813.

33 Mulugeta W, Hoque L. Impact of the COVID-19 Lockdown on Weight Status and Associated Factors for Obesity Among Children in Massachusetts. Obesity Medicine;22(6):100325. Available from: https://doi.org/10.1016/j.obmed.2021.100325.

Supplementary Materials for "Transient Buffering Effects of Parks Accessibility Against Movement Control Policies on Child Weight Status: A Quasi-Experimental Analysis in Singapore" (January 6, 2026)

Table of Contents

A. Data Appendix

This data appendix summarizes key data and data merging to arrive at the final individual-calendar year panel data used in the main analyses.

- *Geocoding cohort residential data.* We use participants' geocoded residential records as the key connecting thread between individual-level and environmental measures (e.g., parks). From over 1,450 recruited pregnant women, the cohort eventually had 1217 successful live births based on the observed infant date of birth, from whom we retrieved residential traces through the years. We use only the postal code part of residential addresses (other components are masked), where we have n = 14,344 of such observations spanning 2010–2022. We geocode the postal codes for the geographical coordinates (latitude, longitude) using OneMap (https://www.onemap.gov.sg/apidocs/search). We successfully geocoded all postal codes except for 18, which are not found in the official and government-operated OneMap archive. The cohort changed the subject identification number format a few years after inception (from without to with zero-padded numbers for the last component), and we enforce a normalized ID number across all years for clean merges by ID.

- *Geographical representation and distribution.* We use the geo-coordinates of addresses to spatially map to all other spatial data, including the official Master Plans (https://www.ura.gov.sg/Corporate/Planning/Master-Plan) for the region, planning areas, and subzones, which are official delineation for urban planning and census taking. We observe at least one residential trace for 1,216 children, spanning 2022 residential points across 64 postal sectors, 24 postal districts, 36 planning areas, and 185 subzones.

To validate that the cohort is geographically representative of the national population, we map the geographical distribution of cohort participants to the 2010 decennial census[15]. We restrict census counts of the population by planning areas and subzones to women aged 20–50, which is the age range of the GUSTO mothers at recruitment (also around 2009-2010). At the planning area level, the correlation coefficient between GUSTO participants and the census population is 0.95 ($p < .001$), with a 95% bootstrapped ($n = 10,000$) confidence interval (CI) of 0.93–0.97. At the subzone level, the correlation remains high at 0.93 ($p < .001$), with a 95% bootstrapped CI of 0.90–0.95[16]. Overall, these results indicate a strong alignment between the spatial distribution of the cohort and the general Singapore residential population.

- *Tracing cohort residence across time.* All recorded dates in the postcode history are linked to the child's birth date to trace a child's residence over time. Each residential record is then assigned the corresponding child's exact age in days at the time of the record. From this, every year at the child's birthday, we identify the residential record before the birthday that is closest to the birthday[16]. The precise method for linking residential records to each year y of a child's age (A) is:

$$\text{residence}_y = \text{residence}_{t^*} \quad s.t. \quad t^* = \max\{t | A_t \leq y\},$$

where residence at year $y \in \{0, \cdots, 11\}$is based on the record at time t^* when A_t is the child's precise age in years when the residential record was updated.

We observe moving, or within-city migration, when the postal code changes between addresses. A substantial proportion ($\sim$ 57%) of the cohort moved at least once within our observe time frame of residential addresses. Most movers move far away: with 82% moving away from their first observed origin neighborhood (subzone), 76% moving way from their first observed postal sector, for a average distance of 5.9 km with over half moving at least 4 km away. A minority a serial movers who moved more than once, making up 22% of the population. We restrict our main sample to those who moved at most once[10].

- *Travel time.* The starting point for the commute time data starts with representing the Singapore island as a grid of hexagons using the H3 hexagonal hierarchical geospatial indexing system developed by Uber (see https://github.com/uber/h3)[15,16].

We use resolution 9, with a level of precision of approximately 0.11km^2 with an average hexagonal side length of 200m. For comparison, a Geohash of length 6 under the alternative Geohash geocoding system has an area of approximately 0.73km^2 and side lengths of approximately 1.2km by 0.6km.

We use the H3 grid system since our construct of built environments entails a notion of accessibility. Other than finer levels of resolution, each cell in the hexagonal grid system

has only one type of neighbor as defined by the centroid-to-centroid distance (or that there are only edge neighbors in H3 while GeoHash rectangles also have vertex neighbors).

For this iteration of our study, we have about 2.4k hexagonal grids. In total, there are around 9k H3-9 hexagonal grids of resolution 9 in Singapore. Most of these hexagons overlay with the sea, water catchment, and nature reserves. Some also overlay with areas with low residential count. We focus on only H3-9 hexagonal grids overlaying with areas with dense residence—retaining only H3-9 hexagons where their centroid falls within planning areas with at least 10,000 residents (unless the planning area is central) and within subzones with at least 5,000 residents (unless the subzone is central. This yields the 2.4k cells. From this, we get around 2.87 million pairs of H3-9 cells. We then query HERE Technologies (see https://developer.here.com/[17]) to get the commute time between the 2.87 million centroid-pairs. HERE calculates travel durations over a detailed digital map using optimized pedestrian and traffic routing algorithms. As typical with modern routing technologies, the underlying metrics considers path connectivity, walking infrastructure, and typical impedances based on historical travel conditions. Additionally, commute time between points are estimates based on parameters including walking speed and expected public transit waiting times (assuming that public transport service providers adhere to their own timetables).

- *Measuring access to parks*. To measure the number of parks within a very short journey (10 minutes) from the house, we combine the travel time data with annual land zoning data based on urban planning[15,16]. For each year, we restrict the land zoning data to those classified as "Parks", which are described as "areas used or intended to be used mainly for parks or gardens for the enjoyment of the general public and includes pedestrian linkages" in the land use master plans (https://web.archive.org/web/20240120014725/https://www.ura.gov.sg/-/media/Corporate/Planning/Master-Plan/MP19writtenstatement.pdf). Since we restrict travel time to only 10 minutes, the areas accessible within 10 minutes are predominantly places accessible by walking. Walking speeds used in computing travel time are conservative, with the speed parameter set at 1 meter per second / 3.6 kilometers per hour / 2.23 miles per hour, equivalent to approximately 600 meters in 10 minutes, aligning with the slower walking speed of children.

  Finally, we link the residential traces, travel time, and parks data as follows. First, for each residential point in the data, we identify the relevant hexbin containing the residential point using the geocoordinates of postal code. This gives the "home" cell. We then retrieve all other cells that are within 10 minutes of the home cell by the centroid-to-centroid travel time required. We then overlay these accessible areas with the map of parks, quantifying how many of the land zones classified as parks intersect with the areas accessible within 10 minutes.

- *Anthropometric and body composition.* Anthropometric measurements were conducted during the main clinic visits in the GUSTO cohort.[14] In total, across 12 cohort waves and 15 years (2010–2024), we had 21,985 weight observations using calibrated weighing scales and 21,871 standing height observations using stadiometers (recumbent length in infancy/toddlerhood using mobile measuring mats) for 21,846 complete weight-height tuples for 1,178 children (Figure A1). The measurements were recorded with the child's age (in days) on the day of measurement. The measures come with the child's age in days the date when the measure is taken. We link this to the child's birthdate to get the precise date of all anthropometric measures. To build the calendar year (as opposed to GUSTO year) panel of body composition measures as follows. We start by combining all height and weight measures into one long dataset, indexing by the child ID and calendar date. Height is not available before the child turned 24 months old, only length is available, which we use in place of height for those earlier periods. Some children in some calendar years, especially earlier ones from infancy to toddlerhood, have multiple clinic visits, while others, especially in later years, have none.

  To go from the long panel of irregular observations to one with a regular calendar year cadence, we proceed in two steps. For the minority of observations where, in a calendar year, a child has no weight or height measure, we impute what those measures would have been on the last day of the year by linearly interpolating against the child's age in days using the two closest observed measures before and after the date. From this, we obtain 21,846 complete weight-height tuples for 1,177 children. We restrict this to interpolation, so we never extrapolate beyond the earliest and latest observed measurement for a child in the original long data. Approximately 10.9% of the panel observations are interpolated (see the wide two-period estimator that does not rely on interpolation). We also restrict to participants who moved at most once in the entire observed residential trail, giving n = 964 children included in the final panel[10]. Finally, we take the latest measure in each calendar year (not the cohort "year" or wave) for a regular individual-year panel. We then link the panel of BMI data to the panel of parks to arrive at the final panel data of 9,984 child-year observations for 964 children across 15 years from 2010 to 2024. 2024 has only 117 observations, which we bin into 2023 in the DiD estimation, and does not otherwise affect the results[16].

  To compute zBMI measures, we use the World Health Organization (WHO)'s Child Growth Standards. Specifically, for ages 0–5 we use the WHO's `anthro` *R* package (https://github.com/WorldHealthOrganization/anthro), and for ages above 5, we use WHO's `anthroplus` *R* package (https://github.com/WorldHealthOrganization/anthroplus), which provides zBMI for 5–19 years old[23]. We do not examine the weight-for-age z-scores as those are only available until age 10.

- *Closest clinic visits before and after COVID-19 lockdown.* An alternative difference-in-differences estimator uses a two period sample using observations before and after the first lockdown in Singapore. Figure A4 plots the number of clinic visits from Jan 2019 to Jan 2022. The first and biggest lockdown (COVID-19 Circuit Breaker, or, CCB) in Singapore took place from April 7 to Jun 1 of 2020, indicated by the vertical red bar. The same figure confirms that there were no clinic visits during this lockdown. Subsequent small lockdowns are also shaded. To build two period sample, we take the closest observations in time before and after the first lockdown[19].

- *Geographical distribution of residential park access.* Figure 1b plots the average estimated residential access to parks in 2020 using a comprehensive census of residential addresses in Singapore. Specifically, we infer the universe of residential points by combine data from two administrative sources: first, approximately 12,500 residential blocks provided by the Housing & Development Board (HDB), covering the majority of Singapore's public housing; second, around 1,400 dwellings from the Singapore Land Authority (SLA), which captures private residential units and landed properties. Residential locations are geocoded based on postal codes or building centroids. We then compute each point's access to park before aggregating up to the 0.1 km^2 hexagonal spatial bins. We extract two non-participant residence as illustration, with the street-level photo from publicly submitted photos available on Google Maps.

- *Community Mobility Reports.* To contextualize behavioral changes during the COVID-19 pandemic, we incorporate mobility trends from Google's COVID-19 Community Mobility Reports in Figure A2, which track daily changes in visits to location categories relative to a pre-pandemic baseline. The pre-pandemic baseline is defined as the median value for the corresponding day-of-the-week during the five-week period January 3 to February 6, 2020[14,24,25]. The reports include mobility trends to six broad categories of places of interests: Retail & recreation (restaurants, cafes, shopping centers, theme parks, museums, libraries, and movie theaters), Grocery & pharmacy (grocery markets, food warehouses, farmers markets, specialty food shops, drug stores, and pharmacies), Parks (national parks, public beaches, marinas, dog parks, plazas, and public gardens), Transit stations (public transport hubs such as subway, bus, and train stations), Workplaces, and Residential. We focus on two categories relevant to our study: Parks and Transit stations. The time series span from February 15, 2020, to October 15, 2022. To smooth daily fluctuations and highlight longer-term behavioral patterns over the entire sample period, we apply a 14-day moving average to the percent change series, using a rolling window with a minimum of one observation to retain early data points.

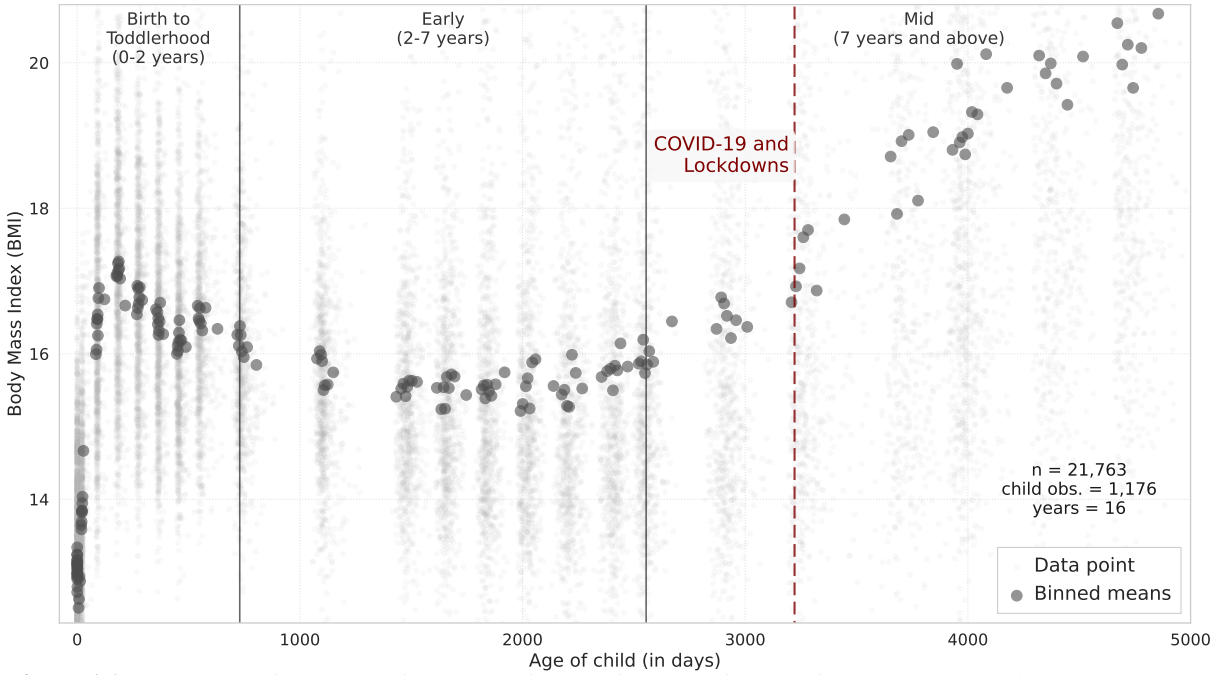

Figure A1|BMI observations (small light grey points) against the child's age in days. Larger dark gray markers are binned means (n = 200), where each bin represents approximately 100 observations. The red dashed line marks the age of the youngest child in the cohort when the WHO declared COVID-19 a global pandemic.

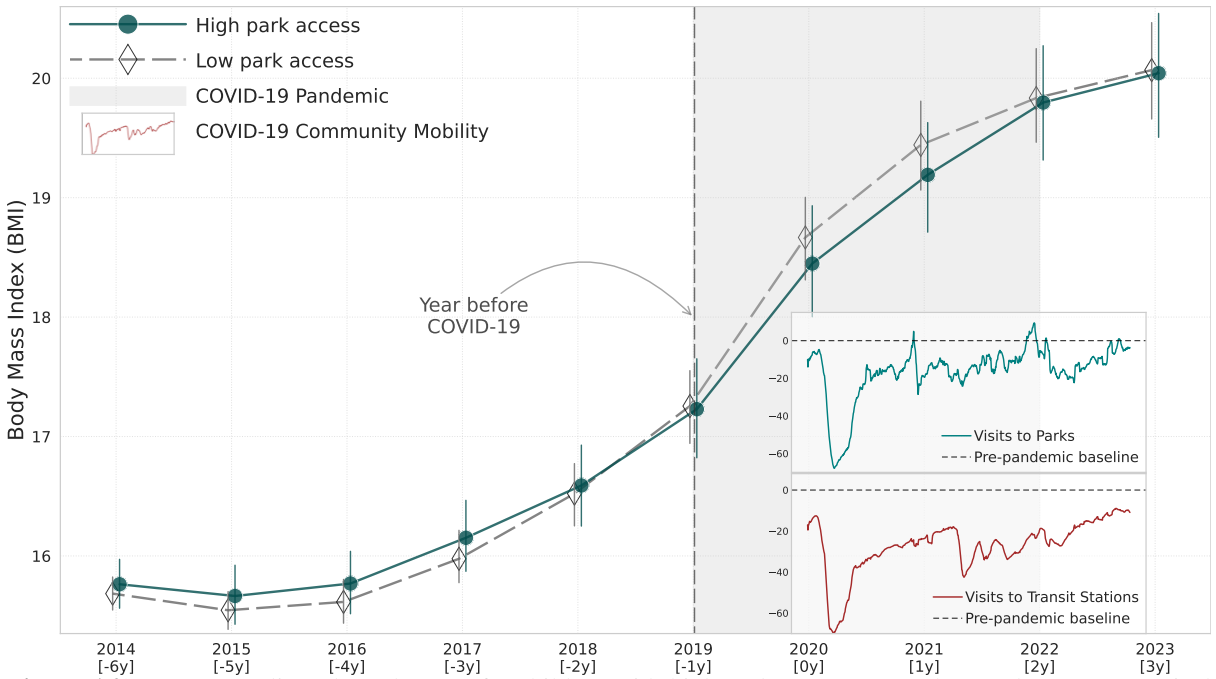

Figure A2|Average unadjusted yearly BMI for children with high park access versus low park access. Vertical lines are 95% bootstrapped confidence intervals. Insets show COVID-19 Community Mobility trends from Google (Appendix A) for visits to parks (top) and transit stations (bottom), aligned to the same time axis. The gray area bookends 2020–2021, when movement restrictions were in place. Brackets indicate years relative to the start of COVID-19 in 2020.

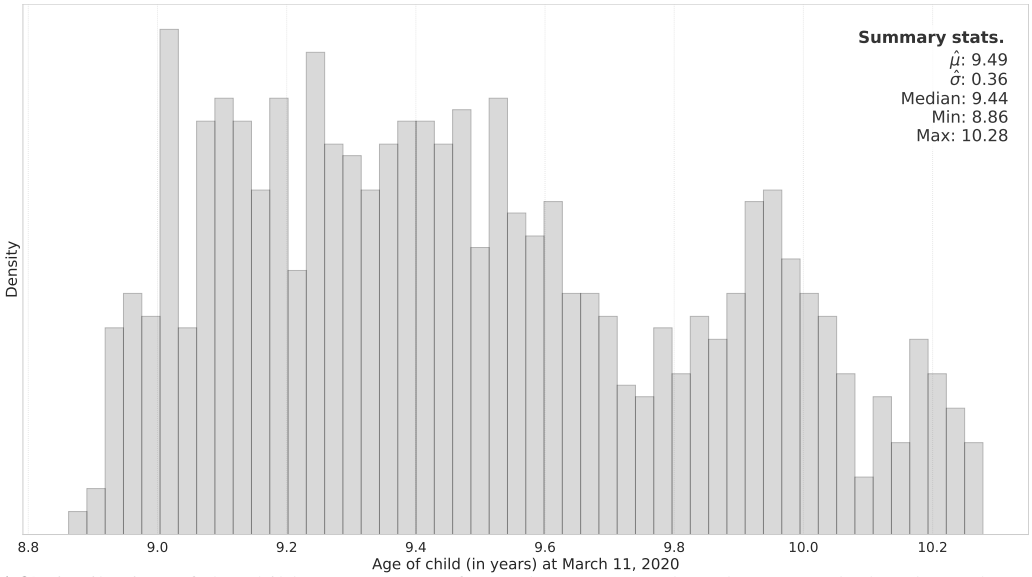

Figure A3|Distribution of the children's ages as of March 11, 2020 when the WHO declared novel coronavirus (COVID-19) outbreak a global pandemic. We take the time delta between each child's birth date and March 11, 2020, and convert days to years. Summary statistics of age is reported in the figure.

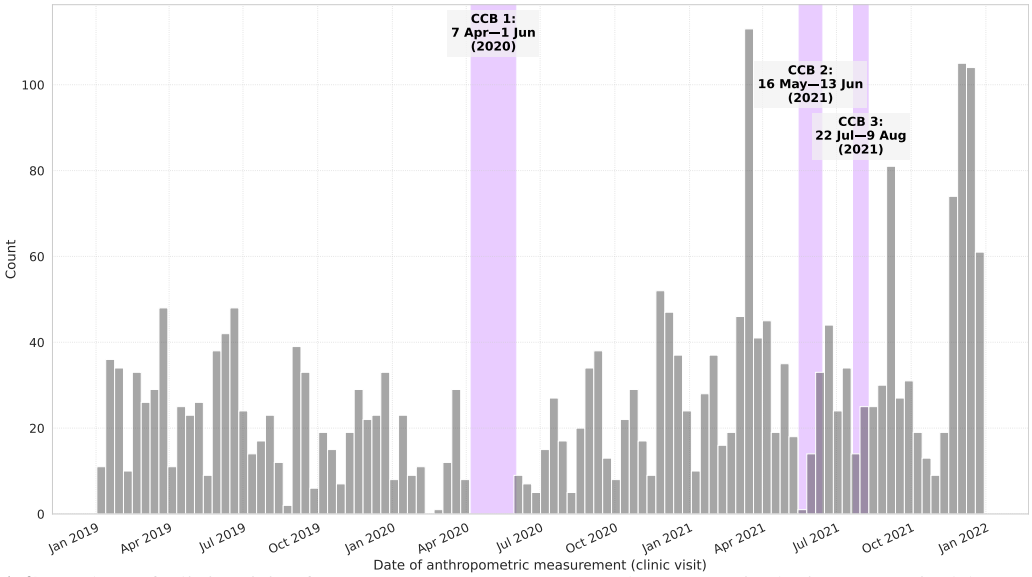

Figure A4|Number of clinic visits from January 2019 to December 2021 (inclusive). Vertical bars show the number of visits by date. The purple shaded areas mark three COVID-19 Circuit Breakers (CCBs), which involved intensified public health measures: CCB 1 (7 Apr–1 Jun 2020), CCB 2 (16 May–13 Jun 2021), and CCB 3 (22 Jul–9 Aug 2021). Each CCB corresponds with a noticeable drop in clinic visits.

B. DiD Design, Assumptions, & Estimation

This appendix lays out the difference-in-differences design, assumptions, and estimation, starting with the potential outcomes definition[7,13], the causal estimand defintion, the assumptions, before connecting the observed quantity to the causal quantity based on the identifying assumptions.

Outcomes

In the simplest setup, we observe outcomes for two periods, $t = 1$ (pre-treatment) and $t = 2$ (post-treatment). A binary treatment indicator $D_i \in \{0, 1\}$ indicates whether unit i is treated. Each unit has two potential outcomes in each period: $Y_{it}(1)$ if treated, and $Y_{it}(0)$ if untreated. The observed outcome is:

$$Y_{it} = D_i Y_{it}(1) + (1 - D_i) Y_{it}(0). \tag{B1}$$

The causal estimand of interest is the average treatment effect on the treated (ATT) in the post-treatment period[19,20,22,22], defined as:

$$\tau_2 = \mathbb{E}[Y_{i2}(1) - Y_{i2}(0) \mid D_i = 1]. \tag{B2}$$

Assumptions

Recovering ATT from data requires identifying assumptions[19,20,22,22]. The first assumption is the stable unit treatment value assumption, or SUTVA, where each unit i's outcome is independent of any other unit's ($j \neq i$) treatment status[4,19]. This is assumption is embedded in Equation (B1).

The second is no anticipation,

$$\mathbb{E}[Y_{i1}(0) \mid D_i = 1] = \mathbb{E}[Y_{i1}(1) \mid D_i = 1], \tag{B3}$$

where in the pre-treatment period, treated units behave as if they have not yet been treated. Or, that outcomes don't start changing for treated group in the pre-treatment period. That is, there is no anticipation of treatment on average. This is a weaker version that only requires it in expectation.

The third is parallel trends between groups,

$$\mathbb{E}[Y_{i2}(0) - Y_{i1}(0) \mid D_i = 1] = \mathbb{E}[Y_{i2}(0) - Y_{i1}(0) \mid D_i = 0], \tag{B4}$$

stating that the trends of the treated had they not been treated is the same as the trends of the control had they not been treated. The latter is fully observed. The former is observed only for

the pre-treatment period ($Y_{i2}(0) \mid D_i = 1]$ is unobserved). We assess the pre-treatment analog of this parallel trend assumption using the event-study specification, as is common [15,16,19,20].

Observed differences to ATT

The three assumptions connect the observed differences to the ATT. We begin with the observed difference-in-differences, differencing the pre-to-post change in the treated group by the pre-to-post change in the control group. We then rewrite the observed outcomes in terms of potential outcomes (Equation (B1)), with the embedded SUTVA assumption. For the treated group, we observe $Y_{i1}(1)$ and $Y_{i2}(1)$; for the control group, we observe $Y_{i1}(0)$ and $Y_{i2}(0)$.

$$
\begin{aligned}
&\underbrace{\mathbb{E}[Y_{i2} \mid D=1] - \mathbb{E}[Y_{i1} \mid D=1]}_{\text{Difference in Treated}} - \underbrace{\mathbb{E}[Y_{i2} \mid D=0] - \mathbb{E}[Y_{i1} \mid D=0]}_{\text{Difference in Control}} \\
&= \underbrace{\mathbb{E}[Y_{i2}(1) \mid D=1] - \mathbb{E}[Y_{i1}(1) \mid D=1]}_{\text{Difference in Treated (PO)}} + \underbrace{\mathbb{E}[Y_{i2}(0) \mid D=0] - \mathbb{E}[Y_{i2}(0) \mid D=0]}_{\text{Difference in control (PO)}} \\
&= \underbrace{\mathbb{E}[Y_{i2}(1) \mid D=1] - \mathbb{E}[Y_{i2}(0) \mid D=1]}_{\tau} \\
&\quad + \mathbb{E}[Y_{i2}(0) \mid D=1] - \underbrace{\mathbb{E}[Y_{i1}(1) \mid D=1]}_{A1} - \underbrace{\mathbb{E}[Y_{i2}(0) \mid D=0] - \mathbb{E}[Y_{i2}(0) \mid D=0]}_{\text{Difference in control}} \\
&= \underbrace{\mathbb{E}[Y_{i2}(1) - Y_{i2}(0) \mid D=1]}_{\tau} \\
&\quad \underbrace{+ \mathbb{E}[Y_{i2}(0) \mid D=1] - \underbrace{\mathbb{E}[Y_{i1}(0) \mid D=1]}_{A1} - \underbrace{\mathbb{E}[Y_{i2}(0) \mid D=0] - \mathbb{E}[Y_{i2}(0) \mid D=0]}_{\text{Trend for control (fully observed)}}}_{\text{Trend for treated had it not been treated}} \\
&= \underbrace{\mathbb{E}[Y_{i2}(1) - Y_{i2}(0) \mid D=1]}_{\tau} + \underbrace{0}_{A2}
\end{aligned}
$$

To isolate the causal effect, we add and subtract the unobserved counterfactual $\mathbb{E}[Y_{i2}(0) \mid D = 1]$, which represents what would have happened to treated units in the post-treatment period had they not been treated, and collect it in τ (Equation (B2)). This step also indicates that observed differences capture the ATT *and* additional differences that potentially cause a bias. For the additional terms to be zeros, we need the no anticipation (Equation (B3)) and parallel trend assumption (Equation (B4)) to hold. Or, that the additional terms sum to zero when the trends for the treated and control group are the same in expectation.

We emphasize that while we test the pre-treatment analog of Equation (B4) in the event-study specification, it is nonetheless an assumption since the potential post-treatment outcome for the treated had it not been treated can never be observed. The above also demonstrates that DiD does not require an absence of selection bias

Importantly, DiD does not require an absence of selection bias[19]:

$$\mathbb{E}[Y_{it}(0) \mid D_i = 1] = \mathbb{E}[Y_{it}(0) \mid D_i = 0],$$

where the pre-treatment outcomes be the same between groups in expectation. However, any bias from selecting into more neighborhood parks must be constant across time, where the difference in outcomes pre-treatment should be the same difference in outcomes post-treatment had treatment not happened for the treated group:

$$\mathbb{E}[Y_{i1}(0) \mid D_i = 1] - \mathbb{E}[Y_{i1}(0) \mid D_i = 0] = \mathbb{E}[Y_{i2}(0) \mid D_i = 1] - \mathbb{E}[Y_{i2}(0) \mid D_i = 0],$$

which is equivalent to Equation (B4) when re-arranged. That is, the nature of the difference between groups does not change over time.

Estimation

We estimate the DiD using our panel data using:

$$\text{BMI}_{it} = \alpha_i + \tau_t + \sum_{p=2010}^{2018} \beta_p \left(D_i \cdot \mathbb{1}\{t = p\}\right) + \sum_{q=2020}^{2023} \gamma_q \left(D_i \cdot \mathbb{1}\{t = q\}\right) + f(\text{Age}_{it}) + \eta_{s(i),t} + \varepsilon_{it}, \tag{B5}$$

where i indexes children and $t \in \{2010, \ldots, 2023\}$ indexes calendar years (as opposed to cohort years/waves). D_i is an indicator for the treated group. τ_t captures time trends shared across all individuals, including early childhood developmental stages (Figure A1). α_i captures all observed and unobserved time-invariant characteristics of the child, such as baseline health and socio-economic conditions, including family income, ethnicity, and genetic endowments, such as predisposition to weight gain[10,20], as typically used in two-way fixed effects estimations of DiD[19,22]. Equation (B5) includes a flexible adjustment of the child's age in days at the clinic measure as a second-degree polynomial, allowing BMI to evolve differently at various developmental stages (Figure A1). $\eta_{s(i),t}$ is neighborhood s's effect allowed to vary across years t to capture neighborhood-wide unobserved trends[9]. ε is the error term, and we clustered the standard errors at the individual to account for within-individual correlation across time for asymptotically valid inference[19,21–23].

We set the baseline year to 2019[15,16,19,20]. $\hat{\beta}_p$ and $\hat{\gamma}_q$ capture the difference between groups in every year relative to the group difference in 2019. Since 2024 has only about 100 observations, we bin them into 2023 as the endpoint[15,16]. The $\hat{\beta}$'s capture pre-COVID differences relative to the difference in 2019, which should all be zero as a pre-event analog test of the parallel trends assumption (Equation (B4)). We analyze BMI, as is, as the main measure, to avoid building in transformation-based artifacts in our outcome, such as with z-scores[8].

Appendix C sketches a model where amenity usage depends on health benefits and access

costs. Health is a function of utility from amenities, which in turn depends on the cost of access (e.g., travel frictions). During the pandemic, rising access costs (e.g., from contracting COVID-19) reduce amenity-driven health benefits differentially, creating variation that maps onto a difference-in-differences design.

C. Model of Amenity Usage

This appendix sketches a simple original model of amenity usage where individuals derive utility from using amenities. The goal is to show that utility from amenities depends on costs from travel outwards, which increases during the COVID-19 pandemic because of costs from violating travel restrictions and the risk of contracting COVID-19, effectively shrinking the feasible set of usable amenities to those very close to home. For those with limited amenities close to home, average utility (e.g., contributing towards health benefits) approaches zero.

Finally, the model connects more directly to the DiD setup.

Utility Framework

We index individuals by i, amenities by a, and year by t (with $t = \tilde{t}$ for COVID years). Each individual (or family) has a universe of amenities $A = \{a_1, a_2, \ldots, a_N\}$. The utility that the individual derives from some amenity a is:

$$u_{ia} = w_i v_a - D(d_{ia}) - \mathbf{1}_{\{t=\tilde{t}\}} \cdot R(d_{ia}). \tag{C1}$$

v_a captures some underlying quality of an amenity (e.g., quality of greenery, degree of novelty, density from the degree of co-usage, and child relevance of a park). w_i is some individual-specific weighting of the qualities of the amenity capturing heterogenous preferences. $D(d_{ia})$ is the cost of traveling a distance d_{ia} from individual i's location to amenity a, including time spent on commute ($D'_d > 0$).

During COVID-19 ($t = \tilde{t}$), an additional cost R arises from travel outwards because of the costs of violating policies that require individuals to stay at home for non-essential activities. Even after these lockdown policies ease, travel outwards is still costly because more time commuting (e.g., higher d_{ia}) increases the risk of contracting communicable diseases like COVID-19 ($R'_d > 0$). For the same amenity a, R means that the utility is much lower during the pandemic: $(u_{ia} \mid t = \tilde{t}) < (u_{ia} \mid t < \tilde{t})$.

An amenity is in the feasible set if its net utility $u \geq 0$, with the set defined as $A_i^* = \{a \in A \mid u_{ia} > 0\}$. Pre-COVID ($t < \tilde{t}$), the costs are determined solely by travel costs:

$$A^*_{i,\text{pre}} = \{a \in A \mid w_i v_a - D(d_{ia}) > 0\}.$$

Post-COVID ($t = \tilde{t}$), the feasible set shrinks due to additional costs from violating policies and the risks of contracting COVID-19:

$$A^*_{i,\text{COVID}} = \{a \in A \mid w_i v_a - D(d_{ia}) - R(d_{ia}) > 0\}.$$

The probability that the individual uses amenity a is:[1]

$$p_{ia} = \frac{\exp(u_{ia})}{\sum_{b \in A_i^*} \exp(u_{ib})}, \tag{C2}$$

where the normalization by the sum of utilities from all feasible amenities reflects the relative attractiveness of amenity a compared to all others. The expected utility for an individual i from all amenities is the sum of utilities weighted by the probability of usage:[2]

$$\mathbb{E}[U_i] = \sum_{a \in A_i^*} p_{ia} \cdot u_{ia}. \tag{C3}$$

Pre- vs. Post-COVID Utilities

Pre-COVID, travel friction (D) were the only disutility. Individuals without nearby amenities (higher minimum values of d) may still derive large positive utilities from distant amenities within the feasible set. For example, a distant park may have interesting features such as park trails, child-friendly playgrounds, and co-play with other children if high density that appeals to the individual or family, which more than makes up for disutilities in commute distance ($w_i v_a > D(d_i a)$). Hence, total utility $\mathbb{E}[U_i]$ does not necessarily suffer for those lacking nearby amenities.

Post-COVID, the additional cost R induces disutilities. Distant amenities (high d_{ia}) are penalized more heavily, shrinking the feasible set to nearby amenities. For individuals lacking nearby amenities, the feasible set may shrink to a null set,[3] effectively reducing their utility to zero. This shuts off any pathways in health benefits that individuals can derive from using amenities (Equation (C4)).

[1]The exponential function ensures non-negative probabilities and allows amenities with higher utility to dominate. The exponential function also reflects random behaviors observed in the real world, allowing individuals to use lower-utility amenities or even negative-utility amenities with vanishingly small probabilities. While this framework theoretically allows for a non-zero probability of choosing an amenity outside the feasible set due to the structure of $\exp(U_{ia})$, the approximation does not materially affect the conclusion that the probability of using far away amenities shrinks after COVID-19.

[2]Pre-COVID ($t < \tilde{t}$), the expected utility is calculated using the pre-COVID feasible set:

$$\mathbb{E}[U_{i,\text{pre}}] = \sum_{a \in A_{i,\text{pre}}^*} P_{ia,\text{pre}} \cdot (w_i v_a - D(d_{ia})) .$$

During COVID-19 ($t = \tilde{t}$), the expected utility accounts for the additional costs of violating policies and the risks of contracting COVID-19:

$$\mathbb{E}[U_{i,\text{COVID}}] = \sum_{a \in A_{i,\text{COVID}}^*} P_{ia,\text{COVID}} \cdot (w_i v_a - D(d_{ia}) - R(d_{ia})) .$$

[3]$A_{i,\text{COVID}}^* = \emptyset \quad \text{if } w_i v_a - D(d_{ia}) - R(d_{ia}) \leq 0 \quad \forall a \in A.$

Connecting to Difference-in-Differences

Some health outcome y (e.g., BMI) depends on the average utility from the amenities ($\mathbb{E}[U_i]$) through some function f:

$$y_{it} = \tilde{\alpha}_i + \tilde{\tau}_t + f(\mathbb{E}[U_i|t]) + \epsilon_{it} \tag{C4}$$

where $\tilde{\alpha}$ is some unobserved time-constant individual-level factor determining health and $\tilde{\tau}$ is some time trend. Since utility U is unobserved, we approximate it through an indicator for whether an individual has access to nearby amenities ($D_i = 1$) and the pandemic years ($\text{Post}_t = 1$):[4]

$$f(\mathbb{E}[U_i|t]) = \theta_i + \theta_t + \phi_1 D_i + \phi_2 \text{Post}_t + \phi_3 D_i \cdot \text{Post}_t + \nu_{it}, \tag{C5}$$

where θ_i and θ_t are baseline constants depending on individual and time, ϕ_1 captures baseline group differences from having nearby access to amenities, ϕ_2 reflects the pandemic-driven reduction in utility U because of the additional pandemic costs (R), and ϕ_3 captures differential reductions in utility from the pandemic between groups. Substituting Equation (C5) in Equation (C4) then yields the estimating difference-in-differences equation for how having nearby access to amenities impacts y during the pandemic:

$$y_{it} = \alpha_i + \tau_t + \beta_1 D_i + \beta_2 \text{Post}_t + \gamma D_i \cdot \text{Post}_t + \varepsilon_{it}, \tag{C6}$$

where γ captures the differential impact of having nearby amenities ($D_i = 1$) after the pandemic ($\text{Post}_t = 1$). $\alpha_i = \tilde{\alpha}_i + \theta_i$ combines the individual-level fixed effects from the health model and utility approximation. $\tau_t = \tilde{\tau}_t + \theta_t$ combines time-specific fixed effects from the health model and utility approximation. The error term $\varepsilon_{it} = \nu_{it} + \epsilon_{it}$ combines residual variation from the utility model and unobserved health shocks.

The dynamic version of the derived two-period DiD Equation (C6) is then the event-study specification Equation (B5) described in Appendix B. The model predicts that differences in health benefits between groups with differential hyperlocal amenity access should return to pre-pandemic norms in COVID-19 recovery years, once the additional costs in Equation (C1) attenuates to 0. Alternatively, habit formation may occur, where the way individuals weigh their subjective utility of amenities (w_i in Equation (C1)) changes because of their experience during the pandemic, in which case differences between groups may persist even after pandemic.

[4] This approximation assumes that $f()$ is linear or that any higher-order interactions and non-linearities in $f()$ are negligible.

D. Supplementary Tables of Main Results

This appendix provides tabulation of the event-study estimates for the main results. The point estimates corresponds to the $\hat{\beta}_p$'s and the $\hat{\gamma}_q$'s from Equation (1). 95% confidence intervals are constructed from standard errors clustered by participants.

Table D1|Estimates of the dynamic difference-in-differences for BMI

Variable	Estimate	Std. Error	95% CI	P-value
2010 x Treated	0.221	0.412	[-0.588, 1.029]	0.592
2011 x Treated	-0.179	0.348	[-0.863, 0.504]	0.607
2012 x Treated	0.068	0.330	[-0.578, 0.715]	0.836
2013 x Treated	-0.014	0.307	[-0.616, 0.587]	0.963
2014 x Treated	0.010	0.290	[-0.558, 0.579]	0.971
2015 x Treated	0.050	0.258	[-0.457, 0.556]	0.847
2016 x Treated	-0.050	0.228	[-0.497, 0.396]	0.825
2017 x Treated	0.007	0.187	[-0.360, 0.374]	0.970
2018 x Treated	0.008	0.127	[-0.240, 0.257]	0.947
2020 x Treated	-0.372	0.153	[-0.672, -0.071]	0.015
2021 x Treated	-0.197	0.204	[-0.597, 0.203]	0.333
2022 x Treated	0.133	0.265	[-0.388, 0.654]	0.616
2023 x Treated	0.022	0.301	[-0.570, 0.613]	0.942
age	0.084	0.069	[-0.051, 0.219]	0.225
I(age^2)	0.002	0.001	[-0.000, 0.004]	0.066
N	9,984			

Note: Corresponds to estimates in Figure 2a.

Table D2|Estimates of the dynamic difference-in-differences for height (cm)

Variable	Estimate	Std. Error	95% CI	P-value
2010 x Treated	-0.118	0.745	[-1.580, 1.344]	0.874
2011 x Treated	-0.553	0.490	[-1.514, 0.408]	0.259
2012 x Treated	-0.587	0.452	[-1.474, 0.301]	0.195
2013 x Treated	0.080	0.416	[-0.736, 0.896]	0.848
2014 x Treated	0.005	0.360	[-0.702, 0.711]	0.990
2015 x Treated	-0.131	0.294	[-0.707, 0.446]	0.657
2016 x Treated	0.089	0.250	[-0.401, 0.579]	0.722
2017 x Treated	-0.145	0.204	[-0.544, 0.255]	0.477
2018 x Treated	-0.104	0.150	[-0.398, 0.189]	0.485
2020 x Treated	0.226	0.244	[-0.254, 0.705]	0.356
2021 x Treated	0.414	0.374	[-0.321, 1.148]	0.270
2022 x Treated	0.117	0.472	[-0.810, 1.043]	0.805
2023 x Treated	0.280	0.590	[-0.878, 1.437]	0.636
age	3.035	0.106	[2.828, 3.243]	0.000
I(age^2)	-0.022	0.002	[-0.025, -0.018]	0.000
N	9,984			

Note: Corresponds to estimates in Figure 2b.

Table D3|Estimates of the dynamic difference-in-differences for weight (kg)

Variable	Estimate	Std. Error	95% CI	P-value
2010 x Treated	0.020	0.775	[-1.500, 1.540]	0.979
2011 x Treated	-0.069	0.661	[-1.366, 1.228]	0.917
2012 x Treated	0.160	0.642	[-1.100, 1.421]	0.803
2013 x Treated	-0.124	0.612	[-1.325, 1.076]	0.839
2014 x Treated	-0.046	0.585	[-1.193, 1.102]	0.938
2015 x Treated	0.191	0.531	[-0.851, 1.233]	0.719
2016 x Treated	-0.114	0.474	[-1.044, 0.816]	0.810
2017 x Treated	0.071	0.383	[-0.681, 0.822]	0.853
2018 x Treated	0.018	0.254	[-0.481, 0.517]	0.942
2020 x Treated	-0.902	0.343	[-1.575, -0.230]	0.009
2021 x Treated	-0.549	0.519	[-1.568, 0.469]	0.290
2022 x Treated	0.219	0.759	[-1.270, 1.708]	0.773
2023 x Treated	-0.009	0.957	[-1.887, 1.868]	0.992
age	-1.642	0.207	[-2.049, -1.236]	0.000
I(age^2)	0.026	0.003	[0.020, 0.032]	0.000
hgt	0.750	0.040	[0.671, 0.828]	0.000
N	9,984			

Note: Corresponds to estimates in Figure 2c.

E. Wide (Two-period) DiD Model

This appendix summarizes results using a wide two-period sample, drawing from observations closest to the lockdown: once before and once after (Appendix A). The estimated model is

$$y_{it} = \delta(D_i \cdot \text{Post-COVID}_t) + \alpha_i + \text{Post}_t + f(\text{Age}_{it}) + \varepsilon_{it}, \tag{E1}$$

similar to the main specification defined in Equation (1), except that there are only two time periods (pre- and post-COVID), as described in Appendix A. We estimate Equation (E1) for four outcomes: BMI, weight, height, and zBMI, reporting estimates in Table E1.

Table E1|DiD estimates using closest observed clinic visit dates

	BMI (1)	Weight (2)	Height (3)	zBMI (4)
Treated group × Post-COVID	-0.224*	-0.583*	0.141	-0.082*
	[-0.469; 0.021]	[-1.17; 0.007]	[-0.246; 0.529]	[-0.178; 0.015]
Age	0.147	-1.06	1.22***	
	[-0.337; 0.632]	[-2.38; 0.256]	[0.319; 2.11]	
Age^2	0.002	0.021**	0.009	
	[-0.005; 0.009]	[0.002; 0.040]	[-0.003; 0.022]	
Height		0.651***		
		[0.522; 0.780]		
# Child	964	964	964	964
# Post-COVID	2	2	2	2
Dependent variable mean	17.5	30.4	127.1	0.311
R^2	0.971	0.985	0.998	0.969
Observations	1,586	1,586	1,586	1,586
Child fixed effects	✓	✓	✓	✓
Post-COVID fixed effects	✓	✓	✓	✓

Note: This table reports estimates from a two period DiD using Equation (E1). Weight is in kg, height is in cm. The weight outcome has an additional adjustment for height. Brackets report 95% confidence intervals with standard errors clustered by individual. Significance levels: * 0.1 ** 0.05 *** 0.01.

F. Supplementary Outcome Measures

This appendix summarizes results for additional outcomes measures related to BMI and weight, estimated using the following specification:

$$y_{it} = \alpha_i + \tau_t + \sum_{p=2010}^{2018} \beta_p \left(D_i \cdot \mathbb{1}\{t = p\}\right) + \sum_{q=2020}^{2023} \gamma_q \left(D_i \cdot \mathbb{1}\{t = q\}\right) + f(\text{Age}_{it}) + \eta_{s(i),t} + \varepsilon_{it}, \quad \text{(F1)}$$

where i indexes children and $t \in \{2010, \ldots, 2023\}$ indexes calendar years, α_i are the child identifiers, τ_t are year trends, $f(\text{Age}_{it})$ is a quadratic in age adjusting for the child's age in days when the measure was taken, and $\eta_{s(i),t}$ are neighborhood (subzone) s fixed effects with a year trend. All estimates are reported as event-study plots[16,19,20]. Each point in the figures is the estimate ($\hat{\beta}_p$ and $\hat{\gamma}_q$) of the difference in y between the treated and control group, relative to the difference in 2019 as the baseline year (year before COVID-19). Capped vertical bars are 95% confidence intervals constructed from standard errors clustered by child. COVID period shaded in gray. Brackets indicate year(s) relative to start of COVID-19 in 2020.

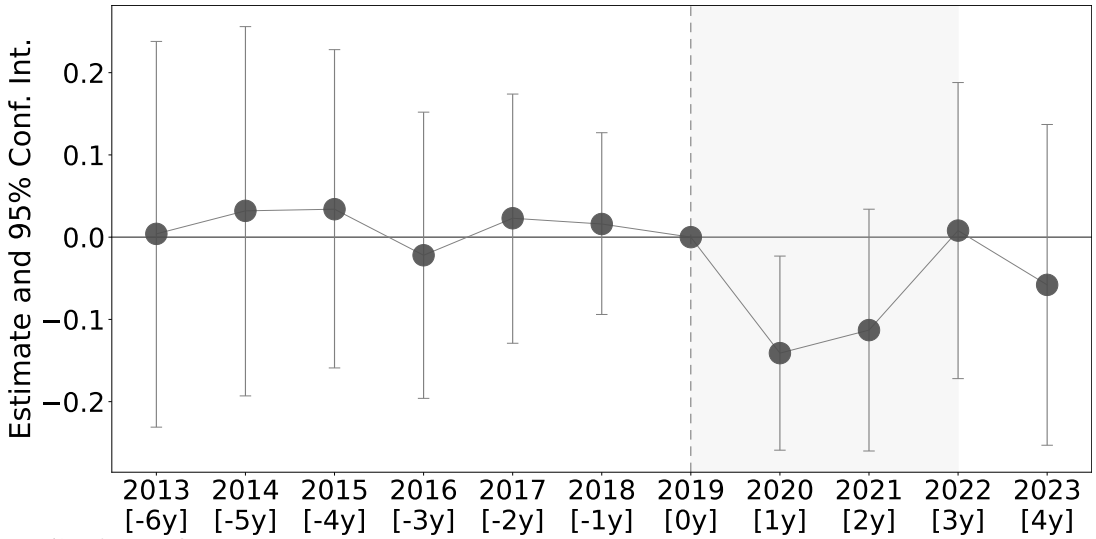

Figure F1|Estimates for zBMI.

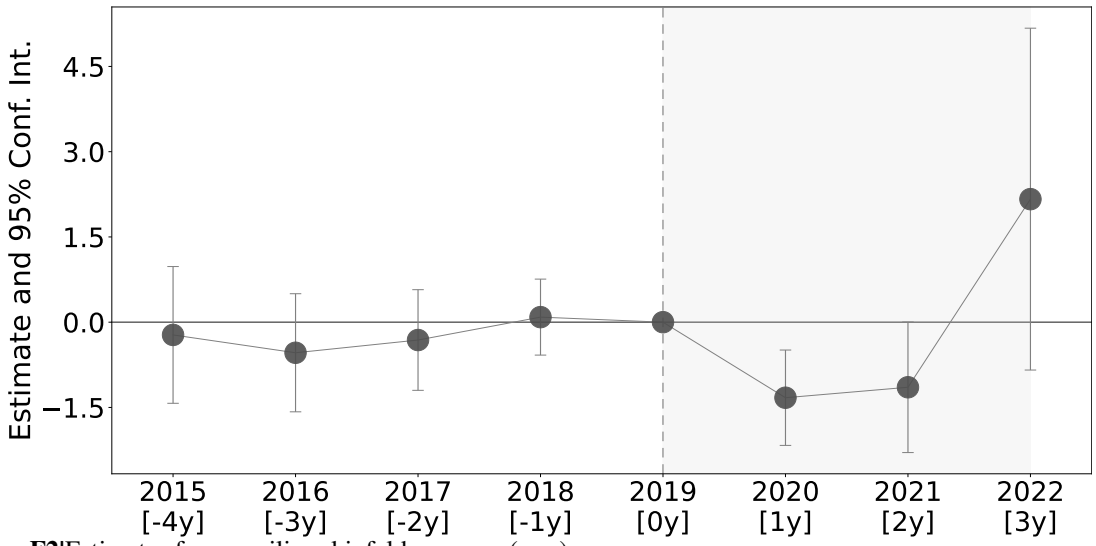

Figure F2|Estimates for suprailiac skinfold measure (mm).

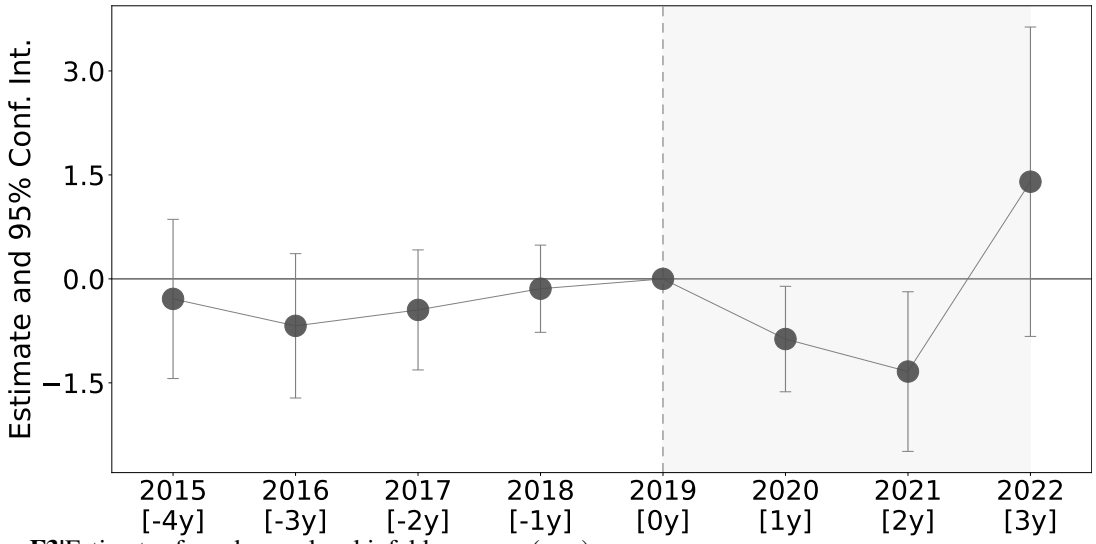

Figure F3|Estimates for subscapular skinfold measure (mm).

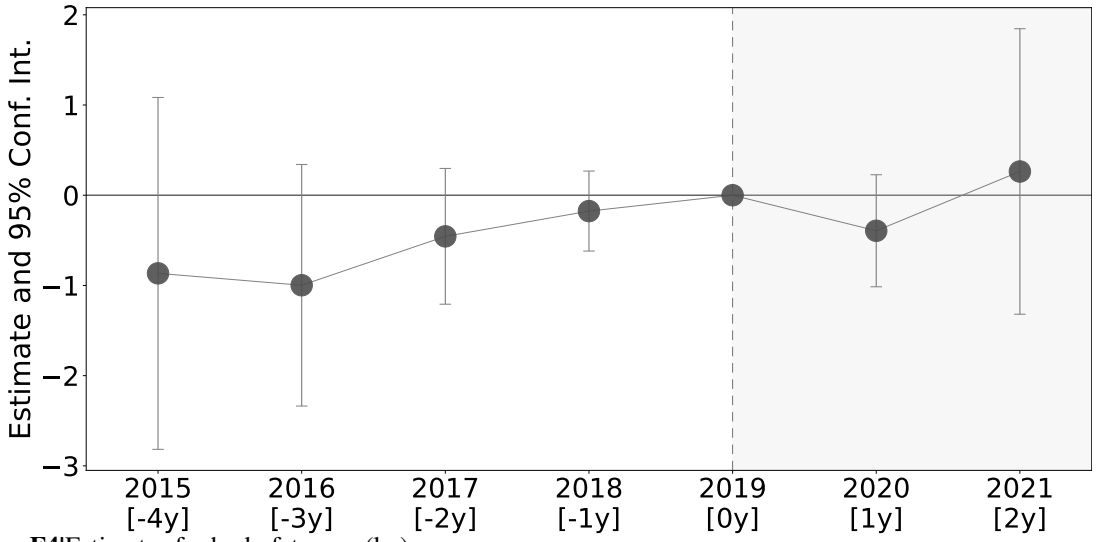

Figure F4|Estimates for body fat mass (kg).

G. Outdoor Play and Exercise

This appendix summarizes results from a subset of the main cohort on outdoor play and exercise before and during the first months of the COVID-19 pandemic.

We link the main panel data to the COVID-19 survey conducted within the same cohort during the pandemic for a smaller group of participants of about 350 children[19]. The survey includes questions on outdoor play, including whether the child plays or exercises outdoors (Every day, Several times a week, Once a week, Less often than once a week, Never), including any activity outside the immediate home *before* the COVID-19 Circuit Breaker (CCB) period (Appendix A). The same question is asked for the CCB period. We code Pre-CCB play and CCB play as 1 if the response is some amount of play and 0 if "Never". We additionally code "Any to none" as 1 if there was any amount of play before the pandemic (Pre-CCB = 1) but no outdoor play at all after COVID-19 (CCB play = 0), and a "Any decrease" as 1 if there is any decrease in reported play and 0 otherwise.

To estimate how the exposure measure relates to outdoor play and changes in outdoor play, we regress the indicators of outdoor play and its change on the treated indicator, adjusting for the child's sex, ethnicity, mother's age, mother's education, household income, and the broader neighborhood region (planning area). We consider this an empirical evaluation of the implicit prediction from Appendix C, where having good proximate residential access to parks should continue facilitating beneficial outdoor play during the pandemic with constrained access to amenities farther away. Children should be more likely to continue outdoor activities if they have parks within a short journey from home.

Table G1 reports the estimates from a smaller subset of n = 310 children. 88% had some outdoor play (and exercise) before the CCB, but this reduced to 57% in the first months of the pandemic. Comparing pre- versus post-CCB reported measures, 64% had some reduction in outdoor play and 34% had a total elimination of outdoor play. Holding the child's and mother's basic demographics, household income, and neighborhood constant, we find evidence that better access to parks relates to a higher probability of play ($\hat{\beta}$ = .101, 95% CI: [−.009, .210]) and lower probability of a total elimination in outdoor play during the CCB ($\hat{\beta}$ = −.127, 95% CI: [−.242, −.013]).

Table G1|Association of outdoor play during COVID-19 and access to parks.

			Changes in outdoor play	
	Pre-CCB play (1)	CCB play (2)	Any to none (3)	Any decrease (4)
High park access	-0.052	0.101*	-0.127**	-0.042
	[-0.133; 0.029]	[-0.009; 0.210]	[-0.242; -0.013]	[-0.160; 0.077]
Male	0.019	-0.002	0.017	0.034
	[-0.038; 0.077]	[-0.107; 0.103]	[-0.076; 0.110]	[-0.075; 0.143]
Ethnicity: Indian	0.066	-0.018	0.076	0.025
	[-0.044; 0.175]	[-0.215; 0.180]	[-0.136; 0.288]	[-0.215; 0.265]
Ethnicity: Malay	0.058	0.008	0.018	0.028
	[-0.017; 0.132]	[-0.165; 0.180]	[-0.184; 0.220]	[-0.113; 0.170]
Ethnicity: Other	0.215***	0.519***	-0.317***	-0.545***
	[0.126; 0.303]	[0.340; 0.697]	[-0.500; -0.134]	[-0.735; -0.354]
Mother's age	-0.001	-0.007	0.003	-0.002
	[-0.010; 0.007]	[-0.017; 0.003]	[-0.005; 0.011]	[-0.011; 0.007]
Mother has college degree	0.061	0.085	-0.028	0.022
	[-0.026; 0.148]	[-0.130; 0.299]	[-0.232; 0.176]	[-0.155; 0.199]
HH income: $1,001–$2,000	-0.052	-0.021	0.057	0.034
	[-0.388; 0.284]	[-0.286; 0.245]	[-0.144; 0.257]	[-0.328; 0.396]
HH income: $2,001–$3,000	-0.053	-0.084	0.061	-0.027
	[-0.363; 0.257]	[-0.326; 0.158]	[-0.147; 0.269]	[-0.247; 0.194]
HH income: $3,001–$4,000	0.127	-0.003	0.160	0.226*
	[-0.174; 0.428]	[-0.336; 0.331]	[-0.068; 0.389]	[-0.011; 0.464]
HH income: $4,001–$5,000	0.151	-0.177	0.334**	0.289*
	[-0.163; 0.466]	[-0.435; 0.081]	[0.079; 0.589]	[-0.007; 0.586]
HH income: $5,001–$6,000	0.174	0.060	0.145	0.189
	[-0.136; 0.484]	[-0.244; 0.364]	[-0.077; 0.368]	[-0.089; 0.467]
HH income: $6,001–$7,000	0.221	-0.178	0.398**	0.342*
	[-0.075; 0.516]	[-0.665; 0.309]	[0.022; 0.774]	[-0.044; 0.729]
HH income: $7,001–$8,000	0.095	0.320*	-0.208	-0.175
	[-0.184; 0.375]	[-0.024; 0.664]	[-0.470; 0.054]	[-0.524; 0.175]
HH income: $8,001–$9,000	0.171	0.012	0.164	0.246
	[-0.145; 0.486]	[-0.377; 0.400]	[-0.183; 0.510]	[-0.074; 0.567]
HH income: $9,001–$10,000	0.183	0.197	-0.007	0.250
	[-0.156; 0.522]	[-0.285; 0.680]	[-0.325; 0.311]	[-0.111; 0.612]
HH income: +$10,001	0.179	0.213	-0.034	0.278*
	[-0.142; 0.500]	[-0.123; 0.548]	[-0.268; 0.200]	[-0.004; 0.561]
# Planning area	29	29	29	29
Dependent variable mean	0.88	0.57	0.34	0.64
R^2	0.20	0.20	0.20	0.18
Observations	310	308	307	307
Planning area fixed effects	✓	✓	✓	✓

Note: *Pre-CCB play* indicates any amount of play before the pandemic. *CCB play* indicates any amount of play during the pandemic. *Any to none* indicates a total elimination of play during the pandemic. *Any decrease* indicates any decline in play during the pandemic. All models are linear probability models. Baseline categories are Female for child's sex, Chinese for ethnicity, no college degree for mother's education, and <$1,000 for household (HH) income. Brackets report 95% confidence intervals with standard errors clustered by the 29 planning areas. Significance levels: * 0.1 ** 0.05 *** 0.01.

H. Other Environmental Measures

This appendix summarizes results from examining other environmental features as alternatives to parks. All event-study specifications remain unchanged from Equation (B5). We first consider other land zoning with potentially similar interpretation as parks. These include Waterbody (water areas for reservoirs, ponds, rivers, etc.), Open Spaces (wooded area, natural open space, etc.), Sports & Recreation (indoor sports complex, swimming complex, golf course, theme park, etc.). We do not observe similar patterns of relative declines.

However, we observe relative declines in BMI for those with above access to land parcels designated for Utility (electric substation, power station, gas installation, etc.), Civic & Community Institution (community centre, community hall, fire station, etc.), Residential, and Residential with commercial at 1st storey as a "mixed" land use type. The last three exhibit visible differences before the pandemic or on a downward pre-trend, although the confidence intervals cross zero.

Secondly, we also consider an alternative measure of parks computed using the total area of parks accessible within a 500-meter radius from the exact residential point, and define treated and control similarly using those above vs. below mean values. We do not observe any significant relative differences.

References (Appendix)

Finkelstein, Amy, Matthew Gentzkow, and Heidi Williams. 2016. "Sources of geographic variation in health care: Evidence from patient migration." *Q. J. Econ.* 131 (4): 1681–1726. 10.1093/qje/qjw023.

Freyaldenhoven, Simon, Christian Hansen, Jorge Pérez Pérez, and Jesse M. Shapiro. 2021. "Visualization, Identification, and Estimation in the Panel Event-Study Design." August. 10.3386/w29170.

Goin, Dana E., and Corinne A. Riddell. 2023. "Comparing Two-way Fixed Effects and New Estimators for Difference-in-Differences: A Simulation Study and Empirical Example." *Epidemiology* 34 (4): 535–543. 10.1097/EDE.0000000000001611.

Goodman-Bacon, Andrew, and Julia Marcus. 2020. "Using Difference-in-Differences to Identify Causal Effects of COVID-19 Policies." *Survey Research Methods* 14 (2): 153–167. 10.18148/srm/2020.v14i2.7742.

Google LLC. 2020. "COVID-19 Community Mobility Reports." https://www.google.com/covid19/mobility/.

HERE Technologies., "HERE Routing API Documentation." https://www.here.com/docs/category/routing.

Holland, Paul W. 1986. "Statistics and Causal Inference." *Journal of the American Statistical Association* 81 (396): 945–960. 10.1080/01621459.1986.10478354.

Leroy, Jef L, Marie Ruel, Jean-Pierre Habicht, and Edward A Frongillo. 2015. "Using height-for-age differences (HAD) instead of height-for-age z-scores (HAZ) for the meaningful measurement of population-level catch-up in linear growth in children less than 5 years of age." *BMC Pediatr.* 15 145. 10.1186/s12887-015-0458-9.

Lim, Jing Zhi, and Lucas Shen. 2022. "Neighborhood Mismatch and Visits." *Research Paper #18-2022, Asia Competitiveness Institute Research Paper Series*, https://www.lucasshen.com/research/nbh-mismatch-visits.pdf.

Rambachan, Ashesh, and Jonathan Roth. 2023. "A More Credible Approach to Parallel Trends." *The Review of Economic Studies* 90 (5): 2555–2591. 10.1093/restud/rdad018.

Ritchie, Hannah. 2020. "Google Mobility Trends: How has the pandemic changed the movement of people around the world?." https://ourworldindata.org/covid-mobility-trends, https://ourworldindata.org/covid-mobility-trends.

Roth, Jonathan, Pedro H.C. Sant'Anna, Alyssa Bilinski, and John Poe. 2023. "What's trending in difference-in-differences? A synthesis of the recent econometrics literature." *Journal of Econometrics* 235 (2): 2218–2244. https://doi.org/10.1016/j.jeconom.2023.03.008.

Rubin, Donald B. 1974. "Estimating causal effects of treatments in randomized and nonrandomized studies." *Journal of Educational Psychology* 66 (5): 688–701. 10.1037/h0037350.

Shen, Lucas. 2020. "Unexpected Shocks to Movement and Job Search: Evidence from COVID-19 Policies in Singapore Using Google Data." *Research Paper #04-2020, Asia Competitiveness Institute Research Paper Series*, https://lkyspp.nus.edu.sg/docs/default-source/aci/aciprp202004.pdf.

Shen, Lucas. 2023. "Does working from home work? A natural experiment from lockdowns." *European Economic Review* 151 104323. https://doi.org/10.1016/j.euroecorev.2022.104323.

Shen, Lucas, Michelle Z.L Kee, Jian Huang et al. 2024. "Parent-specific effects of parks accessibility on child resilience: A longitudinal cohort study."

Shen, Lucas, Subhashni Raj, Youssef Oulhote et al. 2026. "Residential proximity to transport facilities as urban determinants of individual-level per- and poly-fluoroalkyl substance (PFAS) exposures: Analysis of two longitudinal cohorts in Singapore." *Environmental Health*, Accepted.

Soh, Shu-E, Mya Thway Tint, Peter D Gluckman et al. 2014. "Cohort profile: Growing Up in Singapore Towards healthy Outcomes (GUSTO) birth cohort study." *Int. J. Epidemiol.* 43 (5): 1401–1409. 10.1093/ije/dyt125.

Sum, Ka Kei, Shirong Cai, Evelyn Law et al. 2022. "COVID-19–Related Life Experiences, Outdoor Play, and Long-term Adiposity Changes Among Preschool- and School-Aged Children in Singapore 1 Year After Lockdown." *JAMA Pediatrics* 176 (3): 280–289. 10.1001/jamapediatrics.2021.5585.

Wang, Guangyi, Rita Hamad, and Justin S. White. 2024. "Advances in Difference-in-differences Methods for Policy Evaluation Research." *Epidemiology* 35 (5): , https://journals.lww.com/epidem/fulltext/2024/09000/advances_in_difference_in_differences_methods_for.6.aspx.

Wooldridge, Jeffrey M. 2021. "Two-Way Fixed Effects, the Two-Way Mundlak Regression, and Difference-in-Differences Estimators." https://www.researchgate.net/publication/353938385, Preprint, August 16, 2021.

Wooldridge, Jeffrey M. 2023. "Simple approaches to nonlinear difference-in-differences with panel data." *The Econometrics Journal* 26 (3): C31–C66. 10.1093/ectj/utad016.

World Health Organization. 2009. "WHO AnthroPlus for Personal Computers: Manual Software for Assessing Growth of the World's Children and Adolescents." http://www.who.int/growthref/tools/en/, https://cdn.who.int/media/docs/default-source/child-growth/growth-reference-5-19-years/who-anthroplus-manual.pdf.